European Journal of Pharmaceutics and Biopharmaceutics 143 (2019) 35–43

Contents lists available at ScienceDirect

European Journal of Pharmaceutics and Biopharmaceutics

journal homepage: www.elsevier.com/locate/ejpb

In vitro evaluation of *Pseudomonas aeruginosa* chronic lung infection models: Are agar and calcium-alginate beads interchangeable?

Bruna Gaelzer Silva Torres[a], Rana Awad[a], Sandrine Marchand[a,b], William Couet[a,b], Frederic Tewes[a,*]

[a] *Inserm U1070, Université de Poitiers, CHU de Poitiers, 1 rue Georges Bonnet, 86073 Poitiers Cedex 9, France*
[b] *Laboratoire de Toxicologie-Pharmacocinétique, CHU of Poitiers, 2 rue de la Milétrie, 86000 Poitiers, France*

A B S T R A C T

Animal models of chronic lung infection with *P. aeruginosa* (*PA*) are useful tools to improve antibiotic (ATB) treatment. Two main models based on the pulmonary instillation of *PA* embedded in agar or calcium-alginate beads are currently used. However, these two polymers used to prepare the beads have different properties; for example, agar is a neutral polysaccharide while alginate is anionic. We hypothesized that the effect of an ATB on *PA* entrapped in agar or calcium-alginate beads depends on its physicochemical properties, including charge, and concentration. To test this hypothesis, *PAs* were entrapped in agar or calcium-alginate beads dispersed in a growth medium containing either tobramycin (TOB), selected as a cationic ATB, or ciprofloxacin (CIP) selected as a neutral zwitterionic ATB. In vitro, time-kill curves evaluating the efficacy of ATBs over time were performed by measuring the light emitted by a bioluminescent *PA* for 42 h in the presence of ATB concentrations ranging from 0 to 100 times the MIC. In the presence of CIP, time-kill curves obtained with *PA* trapped in agar or calcium-alginate beads were comparable, whatever the CIP concentration used. In the presence of TOB, a clear difference was observed between the kill curves obtained with *PA* embedded in agar or calcium-alginate beads. While *PA* trapped within agar displayed the same susceptibility than the planktonic one, it was unresponsive to TOB for concentrations up to 1-fold MIC when trapped in calcium-alginate. At 10-fold the TOB's MIC, the luminescence emitted by *PA01* in the agar beads was reduced by 95% after 40 h, whereas it returned to the same initial value for *PA01* trapped in alginate-based beads. The reduction in TOB efficiency was even greater when alginate-based beads were dispersed in a mucus-simulating medium. These results show that the agar and alginate beads models can be interchangeable only for uncharged ATB, such as CIP, but not for cationic ATB, like TOB. In vitro experiments performed in this study could be a quick way to evaluate the effect of each model on a given ATB before performing animal experiments.

1. Introduction

Animal models of chronic lung infection with *Pseudomonas aeruginosa* (*PA*) are useful tools to improve antibiotic (ATB) treatment of these infections in human. The first murine model of chronic bronchopulmonary infection with *PA* was developed by pulmonary instillation of *PA* embedded in agar beads [1]. The aim of embedding *PA* within agar beads is to physically restrain the bacteria in the airways by creating an interface between the bacteria and the host that protects them from each other. This leads to persistent stimulation of host defenses and to inflammation that mimics the pathophysiology of chronic lung infection observed in human [2]. A second model was then developed using calcium-alginate beads to replace the agar beads. These alginate-based beads better simulate *in vivo* conditions in which mucoid *PA* are embedded within self-produced alginate found in pulmonary biofilms in cystic fibrosis (CF) patients [3–5].

Both models are still used today to evaluate the efficacy of ATB to treat chronic lung infections [2,4,6–8]. However, these two polymers used to form the beads have different properties; for example, agar is a neutral polysaccharide while alginate is anionic. Thus, they could interact differently with ATBs, especially in relation with their charge, and thereby might alter their diffusion, binding, and as a result their efficacy. Therefore, using TOB and CIP as representatives of cationic and non-ionized ATBs, respectively, the aim of this study was to determine whether these models have an impact on the efficiency of some ATBs or whether they can be considered interchangeable. Indeed, we hypothesized that the effect of an ATB on bacteria entrapped in agar or calcium-alginate beads could depend on its physicochemical properties, such as ATB charge and concentration. To test this hypothesis, *in vitro* time-kill curves-like, measuring ATB efficacy over the time have been performed by recording the light emitted by a bioluminescent *PA* for 42 h for different TOB and CIP concentrations.

2. Methods

2.1. Materials

A *P. aeruginosa PAO1* strain, hereafter referred as *PAO1*, which was

* Corresponding author at: INSERM, U1070, UFR de Médecine Pharmacie, Université de Poitiers, 1 rue Georges Bonnet, TSA 51106, 86073 Poitiers Cedex 9, France.
E-mail address: ftewes@univ-poitiers.fr (F. Tewes).

https://doi.org/10.1016/j.ejpb.2019.08.006
Received 21 May 2019; Received in revised form 31 July 2019; Accepted 12 August 2019
Available online 13 August 2019
0939-6411/

made bioluminescent by chromosomal integration of the luxCDABE operon, was kindly provided by Professor Patrick Plesiat (Centre National de Référence de la résistance aux antibiotiques, Centre Hospitalier Universitaire de Besançon, France). Tobramycin (TOB) and ciprofloxacin (CIP), were purchased from Sigma Aldrich (France).

2.2. Luminescence kinetics using planktonic P. Aeruginosa

PAO1 was grown overnight in cation-adjusted Mueller-Hinton Broth (MHB; Sigma-Aldrich, France) in an orbital shaker at 37 °C. The optical density of a suspension measured at 600 nm (OD_{600}) was adjusted to 0.03 ($\approx 1–2 \times 10^7$ cells/mL)[9] in MHB (after subtracting MHB absorbance value) and the suspension was incubated at 37 °C. Once the exponential phase of growth was reached (approximately 3 h, evaluated by measuring the OD_{600} every 15 min), 100 µL of the bacterial suspension, having a concentration adjusted to obtain an initial luminescence of 10 000 RLU, were dispersed in the wells of a low-binding (to avoid biofilm formation), white, flat-bottom, 96-well microplate (Greiner®, ref: 655904, France). Then, 100 µL of MHB containing the 2 times concentrated ATB was added. ATBs concentrations used, expressed in number of times the minimum inhibitory concentration (MIC; 0.025 mg/L for CIP and 0.5 mg/L for TOB) were 100, 50, 25, 10, 5, 2, 1, 0.5, 0.25, and 0. The plates were sealed with a clear, gas permeable, moisture barrier membrane (4titude®, ref: 4ti-0516/96) and luminescence was recorded every 30 min for 42 h at 37 °C using an Infinite M200 Pro microplate reader (Tecan, France). The use of luminescence enables each well to be used as its own control over time, thus limiting the number of wells required in the study and minimizing well-to-well variations by normalization. Thus, luminescence values recorded at different times were normalized by the initial luminescence recorded for each well so that all kinetics curves start at 1 on the y-axis. Plates were shaken before each measurement (n = 12–16).

2.3. Luminescence kinetics using biofilms adsorbed on an abiotic surface

For biofilms formation, the OD_{600} of an overnight suspension was adjusted to 0.03 in MHB and 200 µL were dispensed in the wells of high-binding (to facilitate bacteria adherence), white, flat-bottom 96-well microplate (Greiner®, ref: 655074, France). Plates were sealed using an air-permeable membrane and incubated in an orbital shaker at 37 °C. After 24 h, the supernatants were removed, and the wells were rinsed 4 times with 150 µL of PBS pH 7.4. The washing procedure is critical, with the main emphasis on preserving biofilm integrity. Then, 200 µL of MHB containing the 1 time concentrated ATB were added. The plates were sealed with a clear, gas permeable, moisture barrier membrane, and then the luminescence was recorded every 30 min for 42 h at 37 °C using the microplate reader (Tecan, France) (n = 12–16). In the presence of planktonic bacteria, the value of the initial luminescence was set around 10 000 RLU in each well by adjusting the bacteria concentration. For biofilms, the initial number of bacteria could not be changed and the initial luminescence values used to normalize the data ranged from 2000 to 5000 RLU.

2.4. Luminescence kinetics using P. Aeruginosa entrapped in polysaccharides beads

2.4.1. Agar beads preparation

Agar beads loaded with *PAO1* were prepared using an adapted version of the method described by Growcott et al. [2]. Fresh *PAO1* suspension prepared in MHB was cultured to exponential growth phase and then adjusted to an OD_{600} of 0.3. Two mL of this suspension was washed with PBS pH 7.4 and bacteria were concentrated in 1 mL of PBS. Then, this suspension was dispersed in 9 mL of 2% m/v molten agar solution (agar; VWR, France), which was then emulsified into 100 mL of warmed (48 °C) paraffin oil (Sigma Aldrich, France) containing 0.01% v/v of sorbitan monooleate (SPAN®60, Sigma Aldrich, France) using a mechanical stirrers model RZR-2021 (Heidolph, France) at 1300 rpm. Then, under moderate mixing (300 rpm), the emulsion was cooled for 1 h by pouring pieces of ice around the beaker to produce agar beads, which were centrifuged at 5000*g* for 10 min, and then washed 4 times with PBS pH 7.4. Sterile beads were prepared under the same conditions by using 1 mL of PBS instead of 1 mL of bacterial suspension and their size distribution was determined by laser light diffraction (Microtrac® X100 particle size analyzer). Evaluations of the size of some *PAO1*-loaded beads were performed by microscopic observation.

2.4.2. Alginate beads preparation

Alginate (Alginic acid sodium salt from brown algae; Sigma Aldrich, France) beads were produced using the same emulsification process than for agar beads preparation. However, after the emulsification step, the gelation of the droplets containing the alginate at a concentration of 2% m/v was induced by adding dropwise and under stirring 20 mL of 0.1 M TRIS-HCl buffer pH 7 containing 0.1 M of $CaCl_2$ to the emulsion. After 2 h of moderate stirring (300 rpm), beads were centrifuged at 5000*g* for 10 min and then washed 4 times with a 0.9% m/v NaCl solution. Sterile beads were prepared by the same method to determine their size distribution.

2.4.3. Time-luminescence kinetics with polymer beads

PAO1 loaded into freshly prepared beads were dispersed in MHB and bioluminescence was adjusted to obtain the same luminescence intensity than with the experiments done using planktonic bacteria ($\approx$10,000 RLU). Then 100 µL of beads suspension was dispensed in a low-binding (to avoid biofilm formation), white, flat-bottom, 96-well microplates (Greiner®, ref: 655904, France), followed by 100 µL of 2 times concentrated ATB solution in MHB. The plates were sealed with a clear, gas permeable, moisture barrier membrane and luminescence was recorded every 30 min for 42 h at 37 °C using the microplate reader (Tecan, France) (n = 12–16).

In traditional *in-vivo* models of *PA* chronic lung infection, polymer beads are instilled into the animal lungs, and after 3–4 days when the bacterial burden is stable, they are exposed to ATB [4]. Under these conditions, biofilms can be created inside the beads before being in contact with ATB [10]. Thus, to evaluate the effect of biofilm formation within the beads, *PAO1*-loaded agar beads were incubated under stirring for 48 h at 37 °C in MHB, and then washed 4 times with PBS pH 7.4. Afterward, the luminescence of the bead suspension was adjusted to 10,000 RLU in MHB and luminescence kinetics were recorded in the presence of various TOB concentrations as described above.

Most of the *PA* chronic lung infections are associated with the presence of abundant mucus which can be an additional barrier to ATB efficacy [11,12]. To test the effect of the components of the mucus on the calcium-alginate beads model, additional luminescence kinetics were performed by dispersing the beads in an artificial sputum medium (ASM) instead of the MHB, in the presence of different TOB concentrations. ASM was prepared following the protocol of Sriramulu et al. [13]. It contains 5 g/L of mucin from porcine stomach (Sigma-Aldrich, France), 4 g/L of low molecular-weight salmon sperm DNA (Sigma-Aldrich), 5.9 mg/L of the iron-chelator diethylene triamine pentaacetic acid (Sigma-Aldrich), 5 g/L of NaCl (Sigma-Aldrich), 2.2 g/L of KCl (Sigma-Aldrich), 5% (v/v) of egg yolk emulsion (Sigma-Aldrich) and 5 g/L of casein amino acids (Sigma-Aldrich).

2.5. Antibiotic diffusion measurements

Effective diffusivities of CIP and TOB within the two gels were determined by assaying the amount of ATB that crossed a layer of gel as a function of time. In these experiments, 2% m/v agar or calcium-alginate gel layers were prepared in membrane-free Thincerts® 24-well plate inserts (Greiner bio-one; France). The thickness of the gel layers was adjusted to 0.45 cm by trimming off the excess of gel. Inserts were placed in a 24-well plate and equilibrated for 1 h at 37 °C with 1.2 mL

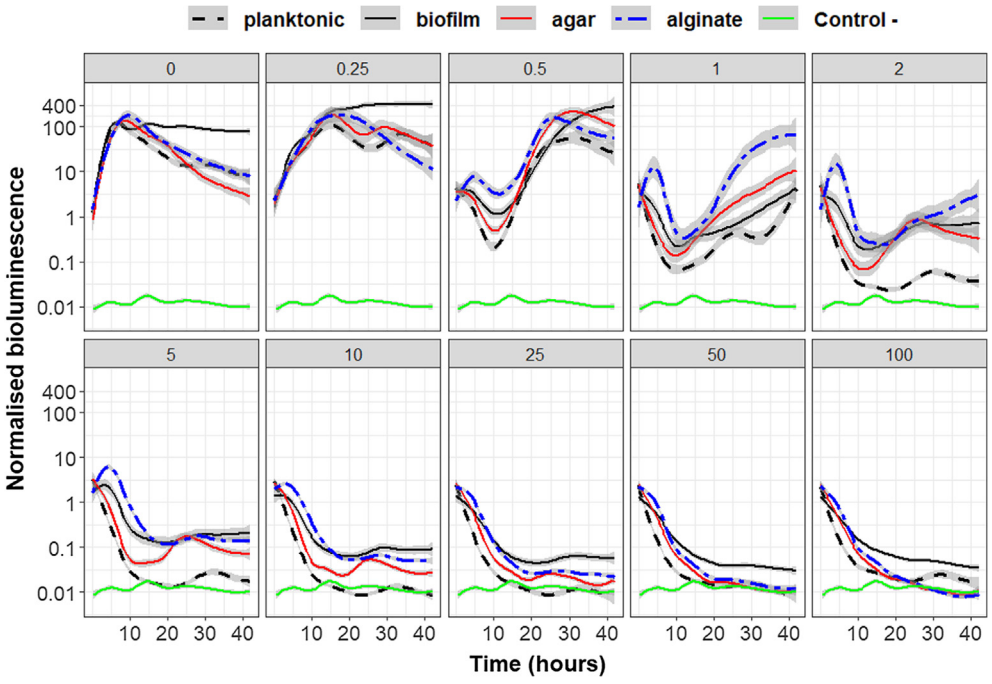

Fig. 1. Time-luminescence curve obtained with planktonic *PAO1* (black dashed lines), biofilms of *PAO1* (black solid lines), *PAO1* trapped in agar beads (red solid lines), or *PAO1* trapped in calcium-alginate (blue two-dash lines) beads exposed to various CIP concentrations in MHB expressed in the number of times the MIC (Top of each graph). The green horizontal curve (Control -) is the signal obtained in the absence of bacteria. For each well, luminescence intensity was normalized to the value measured at time zero. The gray band around the lines is the 95% confidence level interval of the mean values predicted from the GAM smoothing model (n = 6–16). The mean values between different conditions are significantly different in the absence of overlapping of these gray-shaded areas. (For interpretation of the references to colour in this figure legend, the reader is referred to the web version of this article.)

and 0.25 mL of TRIS-HCl buffer pH 7 in the acceptor and donor compartment, respectively. Then, TRIS-HCl buffer in the acceptor compartment was removed and replaced by a TRIS solution containing the ATB at a concentration of 10 or 100 times the MIC. At different times (10, 20, 30, 40, and 60 min for CIP and 30, 60, 90, 120, and 150 min for TOB) 500 µL of the acceptor compartment was removed and replaced by the same volume of warm, ATB free, TRIS buffer pH 7 (n = 4 per ATB concentration). ATBs concentrations were determined using the analytical methods described on Section 2.7. The cumulative amount of ATB per centimeter square (ng/cm^2) versus time was plotted to check linearity and calculate the slope (ng/s/cm^2). Apparent permeability (cm/s) was calculated by dividing the slope by the donor compartment initial ATB concentration (ng/cm^3). Effective diffusivity (cm^2/s) was calculated by dividing the apparent permeability by the gel layer thickness (cm).

2.6. TOB binding to alginate

Calcium-alginate gels were formed by adding 200 µL of alginate solution at 2% m/v in Eppendorf tubes and then, after centrifugation, 600 µL of 0.1 M TRIS-HCl buffer pH 7 containing 0.1 M of $CaCl_2$. After 4 h of gelation, 550 µL of liquid was removed and 500 µL of TOB solution in TRIS-HCl was added. After incubation for 7 days at 37 °C, the free TOB concentration in the liquid phase in equilibrium with the gel was determined by the LC-MSMS method described below. A control without alginate gel was treated in the same conditions to evaluate the TOB stability and plastic tube binding. No significant change in TOB concentration was observed in the control over the 7 days. The data for three experiments on binding of TOB to calcium-alginate gel were analyzed as described by Nichols et al. [14] using a linear adsorption isotherm equation, B = RC, where B is the amount of TOB bound in a unit volume (in µg/mL), C is the free TOB concentration (µg/mL), and R is a constant of proportionality.

2.7. Antibiotic assays

2.7.1. CIP assay

CIP was assayed using an Infinite M200 Pro microplate reader (Tecan, France) as a fluorimeter. Stock solutions of CIP in acidic water with 0.1 mM HCl were prepared at 1 mg/mL. Standard solutions having CIP concentrations of 100, 50, 25, 10, 5, and 1 ng/mL as well as QC solutions having CIP concentrations of 75, 15, and 2.5 ng/mL were prepared in PBS pH 7.4 or TRIS-HCl pH 7. Then, 250 µL of these solutions and samples were added in the wells of a low-binding, white, 96-well microplate (Greiner®, ref: 655904, France) and the fluorescence intensity at 430 nm was measured after excitation at 278 nm. Coefficients of determination of linear regressions of calibration curves were higher than 0.99 and QC and standards biases were lower than 15%.

2.7.2. TOB assay

TOB was assayed using an LC-MSMS method previously described [15]. Briefly, a Waters Alliance 2695 separation module coupled with a Waters Micromass Quattro micro API tandem mass spectrometer was used. Chromatographic separation was done with an X bridge C18 column (5.0 µm, 150 by 2.1 mm); Waters, St-Quentin en Yvelines, France) and a mobile phase composed of 0.1% (vol/vol) formic acid in water and 0.1% formic acid in acetonitrile (75:25, vol/vol) flowing at 0.2 mL min^{-1}. Quantification was performed in the positive-ion mode with multiple-reaction monitoring of *m/z* transitions 468.2 → 163.1 for TOB and 448.2 → 160.2 for sisomycin, the internal standard (1 µg/mL). TOB concentrations of the standard solutions were 1000, 750, 500, 100, 25, 5, 2.5, and 1 ng/mL and 750, 100, and 2.5 ng/mL for the QC solutions. Coefficients of determination of linear regressions of calibration curves were higher than 0.99 and QC and standards biases were lower than 15%.

2.8. Data analysis

All data analyses were performed using the R software version. 3.4 and the package “ggplot2 v. 3.10” was used to plot smoothed mean luminescence values versus time using a generalized additive model (GAM) as smoothing method. The shaded area around the mean value curve is the 95% confidence level interval for the mean values predicted from the GAM smoothing model.

3. Results

Bioluminescence kinetics of planktonic *PA* and adsorbed biofilms of *PA* in the presence of CIP or TOB. In order to obtain references for

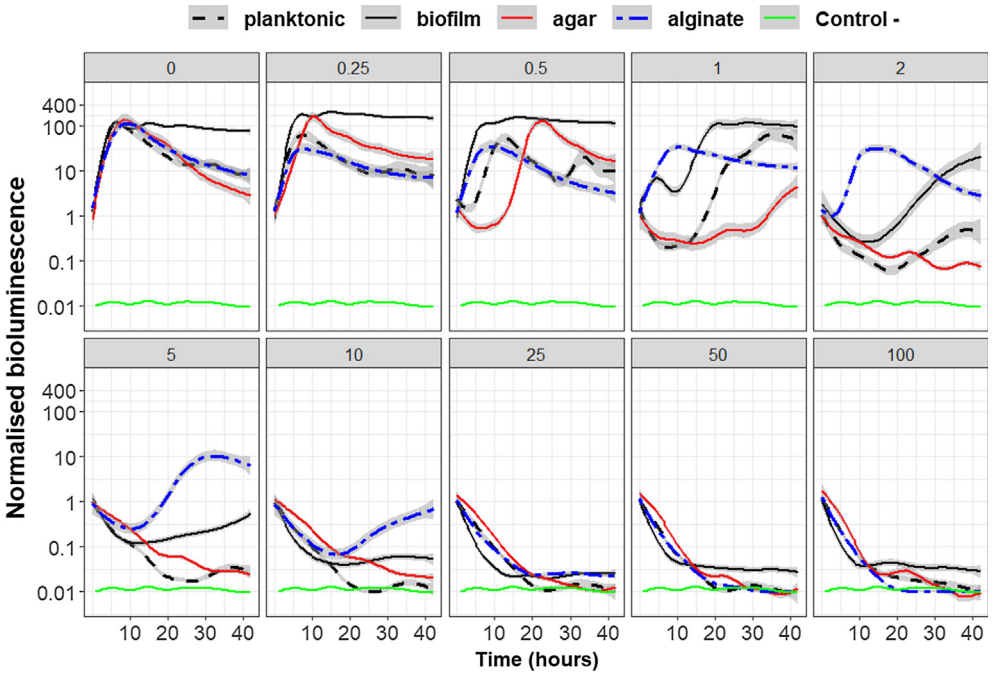

Fig. 2. Luminescence kinetics obtained with planktonic *PAO1* (black dashed lines), biofilms of *PAO1* (black solid lines), *PAO1* trapped in agar beads (red solid lines), or *PAO1* trapped in calcium-alginate (blue two-dash lines) beads exposed to various TOB concentrations in MHB expressed in the number of times the MIC (Top of each graph). The green horizontal curve (Control -) is the signal obtained in the absence of bacteria. For each well, luminescence intensity was normalized to the value measured at time zero. The gray band around the lines is the 95% confidence level interval of the mean values predicted from the GAM smoothing model (n = 6–16). The mean values between different conditions are significantly different in the absence of overlapping of these gray-shaded areas. (For interpretation of the references to colour in this figure legend, the reader is referred to the web version of this article.)

comparing the data obtained with PAs trapped in polymer beads, luminescence kinetics were first recorded for planktonic PAs and PAs adsorbed on plastic surfaces as biofilms in the presence of CIP (Fig. 1) or TOB (Fig. 2).

In the absence of ATB, luminescence produced by planktonic *PAO1* or biofilms of *PAO1* increased similarly for 5 h (Figs. 1 and 2). For biofilms, the luminescence was then stable for the time of the experiment, while it decreased slowly for the planktonic bacteria. The addition of CIP at a low concentration, e.g. 0.25 times the MIC, decreased the bacteria growth rate in both growing mode and a plateau was reached only after 15 h. At this CIP concentration, biofilms had higher normalized luminescence at the plateau compared to values got without ATB. For CIP concentrations comprised between 2 and 100 times the MIC, biofilms formed on the bottom of 96-well plates were less susceptible to CIP than the planktonic bacteria (Fig. 1). A higher luminescence decrease rate and a greater extent of the luminescence decrease were obtained with the planktonic bacteria compare to biofilms.

The overall time-luminescence profiles obtained with CIP or TOB against planktonic or biofilm of *PAO1* were similar and planktonic bacteria were generally more susceptible to both ATBs than biofilms (Figs. 1 and 2). However, for ATB concentrations below 25 times the MIC, biofilms were less sensitive to TOB than CIP. For example, no effects were observed with biofilms exposed to TOB at concentrations up to 0.5 times the MIC (Fig. 2), whereas CIP showed an effect from 0.25 times the MIC (Fig. 1). In addition, for biofilms exposed to ATB concentrations ranging from 1 to 5 times the MIC, greater luminescence rebounds were observed with TOB than with CIP.

Bioluminescence kinetics of *PA* entrapped in agar or calcium-alginate beads. Both types of beads were prepared using a similar emulsification method and comparable monodisperse size distributions were obtained (supplementary material 1). Their mean diameters of 68 ± 23 µm and 81 ± 27 µm, for calcium-alginate and agar, respectively, were not significantly different ($p = 0.58$, two-tailed *t*-test). Luminescence kinetics acquired with *PAO1* trapped in agar or calcium-alginate beads were nearly similar for all tested CIP concentrations (Fig. 1). The only difference observed was an initial increase in luminescence over the five first hours with the alginate beads, while the luminescence decreased immediately with the agar ones for CIP concentrations between 0.5 and 10 times the MIC. Thus, no effect of the polymer forming the beads was observed in the presence of CIP. For CIP concentrations between 0.5 and 10 times the MIC, the luminescence profiles obtained with *PAO1* entrapped in both types of beads were close to those obtained with biofilms adsorbed on the bottom of the 96-well plates. However, for higher CIP concentrations, the profiles were similar to those obtained with planktonic bacteria.

Although no effect of the type of beads used was observed on the CIP effectiveness, for certain TOB concentrations, the luminescence profiles were changed depending on the type of beads. For TOB concentrations lower than 0.5 times the MIC, and higher than 25 times the MIC, no effect of the polymer was observed and the same profiles were obtained with agar or calcium-alginate beads (Fig. 2 - Supplementary materials 4). For these TOB concentrations ranges, the kinetics were similar to those obtained with planktonic bacteria. However, between these TOB concentrations, *PAs* entrapped in alginate-based beads were less susceptible to TOB than those entrapped in agar beads. For this TOB concentration range, *PAs* embedded in the alginate beads were also less susceptible to TOB than the bacteria present in the biofilms adsorbed on the bottom of the 96-well plates and the planktonic bacteria.

PAs freshly entrapped in calcium-alginate beads were less susceptible to TOB than those freshly entrapped in agar beads (Fig. 2). However, in *in vivo* experiments, beads are instilled into the animals' lungs and are exposed to ATB only after 2–3 days when the bacterial burden is stable. During this period, *PA01* can form biofilms in the beads that can influence the effect of ATB. To evaluate this, luminescence kinetics using agar beads that did not appear to interfere with the TOB effect, were incubated for 48 h in MHB prior to the addition of TOB. Luminescence kinetics measured from fresh or 48-hours-old agar beads were almost similar (Fig. 3). *PAs* in 48-h-old agar beads were slightly less susceptible to TOB than *PAs* in the fresh beads only for TOB concentration around the MIC. Additionally, *PAs* trapped into fresh or 48-h-old agar beads were around 10 times more susceptible to TOB than *PAs* freshly trapped into calcium-alginate beads.

Effective diffusivity of TOB and CIP in agar and calcium-alginate gels at 2% m/v. To determine whether the decrease in the efficacy of TOB on *PAs* trapped in calcium-alginate beads compared to *PAs* trapped in agar beads could be due to a decrease in TOB diffusion, the effective diffusivity of the two ATBs were evaluated in both gels by measuring their transport rate through a layer of these gels (Fig. 4).

The CIP effective diffusivity values at 37 °C were similar in both gels, with values of $1.5 \pm 0.2 \times 10^{-6}$ cm^2/s and $1.4 \pm 0.4 \times 10^{-6}$

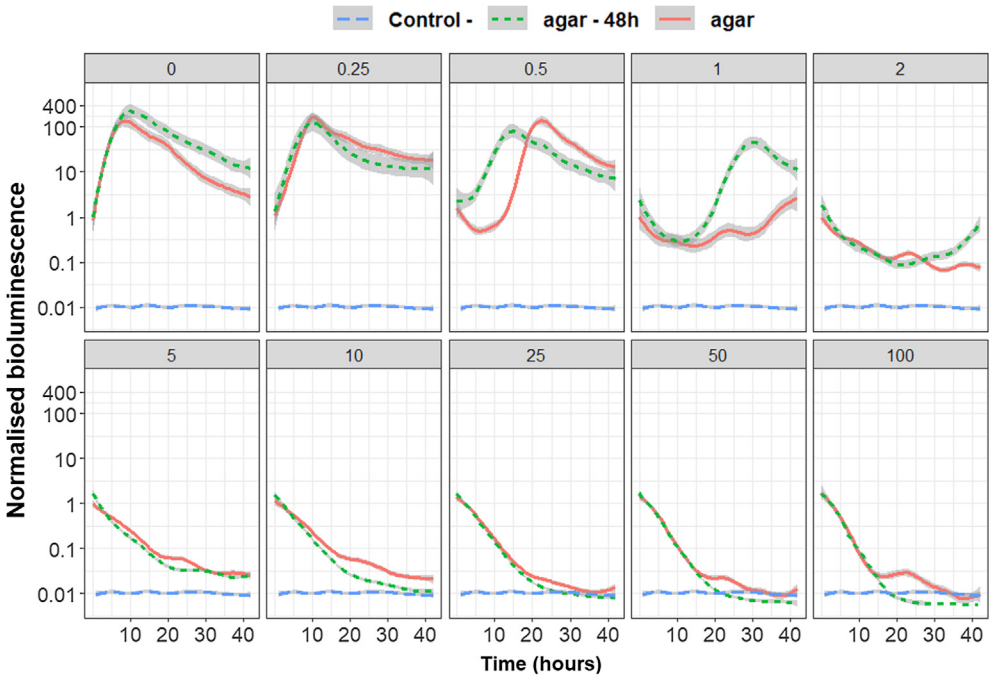

Fig. 3. Luminescence kinetics obtained with *PAO1* freshly trapped in agar beads (solid lines) or for 48 h (dashed lines) before being dispersed in MHB containing different concentrations of TOB expressed in the number of times the MIC (Top of each graph). The blue horizontal curve (Control -) is the signal obtained in the absence of bacteria. For each well, luminescence intensity was normalized to the value measured at time zero. The gray band around the lines is the 95% confidence level interval of the mean values predicted from the GAM smoothing model (n = 12–16). The mean values between different conditions are significantly different in the absence of overlapping of these gray-shaded areas. (For interpretation of the references to colour in this figure legend, the reader is referred to the web version of this article.)

cm^2/s in 2% (m/v) agar and 2% (m/v) calcium-alginate gel, respectively (Fig. 4). TOB effective diffusivity in agar gel ($1.6 \pm 0.7 \times 10^{-6}$ cm^2/s) was similar to that of CIP in this gel. In the calcium-alginate gel, the TOB effective diffusivity was reduced to $0.8 \pm 0.5 \times 10^{-6}$ cm^2/s. TOB interaction with the calcium-alginate gel was further investigated by measuring its binding at equilibrium with this gel. The concentration dependence of the TOB binding to 2% (m/v) calcium alginate gel was linear within the concentration range tested (MIC at 100 times MIC - Fig. 5A), which supposes the absence of saturation. Nichols et al. [14] also found a linear binding of TOB to sodium alginate in this range of TOB concentrations. The constant of proportionality between the amount of TOB bound to alginate and the free TOB concentration was around 3.7.

When adsorption reaches equilibrium instantaneously, solute effective diffusivity (*De*) in a gel can be related to its diffusivity in water by the following equation: $De = D(1/(R + 1))$ [14]. Thus, using the diffusivity of TOB in the water at 37 °C calculated from the Wilke-Chang correlation at 5.6×10^{-6} cm^2/s [16], the effective diffusivity of TOB in the calcium-alginate gel was 1.2×10^{-6} cm^2/s.

Bioluminescence kinetics of *PA* entrapped calcium alginate beads dispersed in MHB or artificial sputum medium. The effect of mucus components on the efficacy of TOB was accessed by measuring the luminescence kinetics of *PA* entrapped in calcium-alginate beads dispersed in artificial sputum medium (ASM) in the presence of different TOB concentrations (Fig. 6). For TOB concentrations of up to 2 times the MIC, no difference was observed in the kinetics obtained with calcium-alginate beads dispersed in MHB or ASM. However, for TOB concentrations greater than 2 times the MIC and up to 50 times the MIC, the ASM components further decreased the efficacy of the TOB compared to the results obtained with alginate-based beads dispersed in MHB. Higher luminescence values were obtained in ASM and rebounds in the luminescence was observed after 40 h for TOB concentrations up to 50 times the MIC.

4. Discussion

Pseudomonas aeruginosa (PA) is responsible for pulmonary chronic infections in patients with chronic respiratory diseases such as cystic fibrosis (CF) and chronic obstructive pulmonary disease (COPD). These *PA* infections are usually associated with the presence of biofilms in the lungs that are impossible to eradicate [5,17,18]. This problem is worsening due to the occurrence of multidrug-resistance (MDR) *PA* worldwide [19]. In this context, new methodologies for treating these pulmonary biofilms are being developed [20]. For example, new therapeutic approaches aim to improve the penetration of ATBs into biofilm/mucus gels by ATB pegylation [12], or by loading them into

A)

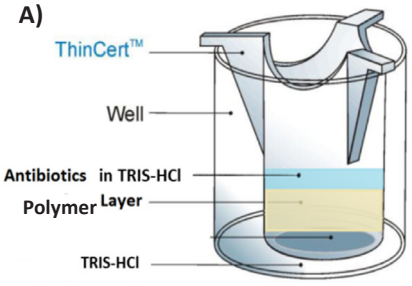

B)

CIP diffusivity in 2% (m/v) agar gel	
Average	1.5 x 10^{-6} cm^2/s
SD	0.2 x 10^{-6} cm^2/s
% of the diffusivity in H_2O	22 % *

CIP diffusivity in 2% (m/v) calcium-alginate gel	
Average	1.4 x 10^{-6} cm^2/s
SD	0.4 x 10^{-6} cm^2/s
% of the diffusivity in H_2O	21 % *

TOB diffusivity in 2% (m/v) agar gel	
Average	1.6 x 10^{-6} cm^2/s
SD	0.7 x 10^{-6} cm^2/s
% of the diffusivity in H_2O	28 % *

TOB diffusivity in 2% (m/v) calcium-alginate gel	
Average	0.8 x 10^{-6} cm^2/s
SD	0.5 x 10^{-6} cm^2/s
% of the diffusivity in H_2O	14 % *

Fig. 4. (A) Scheme showing the test used to determine the ATBs effective diffusivities. (B) CIP and TOB effective diffusivity values measured at 37 °C in 2% (m/v) agar and 2% (m/v) calcium-alginate gels. * The diffusivity percentage of the two ATBs in the gels relative to their diffusivity in pure water was calculated using the diffusivity of the CIP in pure water (6.9×10^{-6} cm^2/s) and the diffusivity of TOB in pure water (5.6×10^{-6} cm^2/s) at 37 °C obtained from Stewart [16].

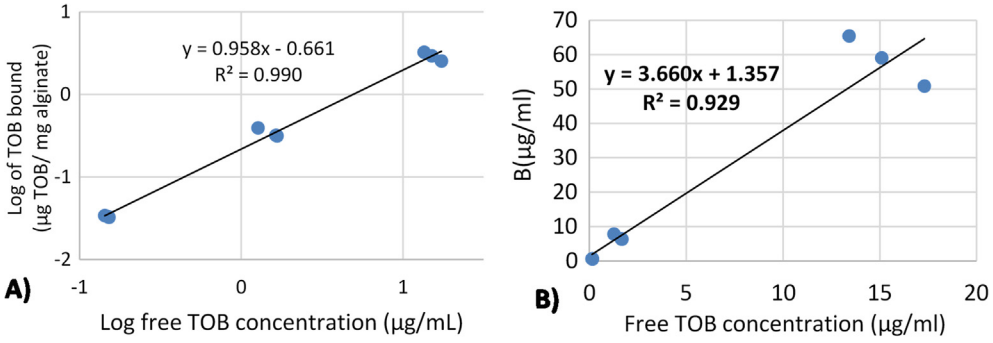

Fig. 5. Measurement of TOB binding to alginate. (A) Log-log plot of the concentration dependence of TOB binding to calcium-alginate gel. (B) Linear TOB adsorption isotherm described by B = RC, where B is the amount of TOB adsorbed in a unit volume (µg/mL), C is the free TOB concentration (µg/mL), and R is the constant of proportionality.

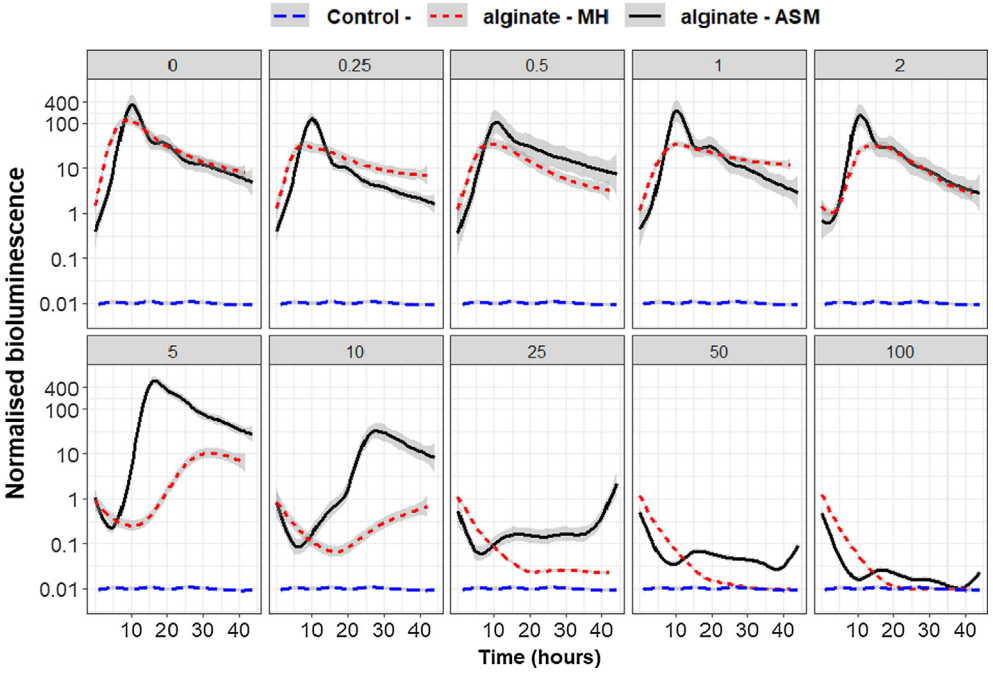

Fig. 6. Luminescence kinetics of *PAO1* obtained for different concentrations of TOB (expressed as a number of times the MIC against planktonic *PAO1*). *PAO1* were entrapped into calcium-alginate beads dispersed either in MH broth (dashed lines) or in artificial sputum medium (ASM) (solid lines). The blue horizontal curve (Control -) is the signal obtained in the absence of bacteria. For each well, luminescence intensity was normalized to the value measured at time zero. The gray band around the lines is the 95% confidence level interval of the mean values predicted from the GAM smoothing model (n = 12–16). The mean values between different conditions are significantly different in the absence of overlapping of these gray-shaded areas. (For interpretation of the references to colour in this figure legend, the reader is referred to the web version of this article.)

nanoparticles able to penetrate these gels [21,22]. Some approaches aim at maintaining high ATB concentration in the lung [23], optimizing ATBs dosage with PK-PD studies [4], or combining several ATBs together or with anti-quorum sensing or biofilm dispersants [24]. To evaluate these strategies, good *in vitro* and *in vivo* models simulating pulmonary biofilms conditions in human are central. The two most common models used to create chronic pulmonary *PA* infections in rodents are pulmonary instillation of *PA* confined in agar beads or calcium-alginate beads. To determine whether these two beads models can be considered interchangeable, *PA*-loaded agar or calcium-alginate beads were challenged with two clinically relevant ATBs, the TOB and the CIP, doing time-kill-like experiments. In order to provide a high throughput-screening test for easy assessment of the ATB efficacy, a bioluminescent *PAO1* was used.

Use of bioluminescent bacteria seems an interesting tool to quickly evaluate the kinetics effect of an antibiotic on bacteria grown either planktonically, as biofilms or immobilized within polymer beads. Time-kill curves are traditionally made by following the variation of concentration of bacteria able to form a colony versus time. This method is time-consuming and allows only a limited number of time points. For biofilms, it is even more complicated as you have to extract the bacteria from the biofilm matrix [12,24]. Monitoring the luminescence produced by transformed bacteria allows live measurements and the acquisition of many points for precise kinetics [25]. Still, bioluminescence is a more complex parameter than a simple bacteria count as its value depends on the concentration of living bacteria but also their metabolic state [26,27]. Yet, bioluminescence permits the observation of living bacteria that are metabolically active but unable to multiply to create a colony, such as bacteria found in biofilms [26,28]. One of the weaknesses of the use of bioluminescence could be the difficulty to access the presence of persisters and ATB tolerant bacteria described in biofilms [29] that have low or almost no metabolic activity and thus should produce much less light than the active bacteria. Anyhow, persisters generally do not produce a visible colony in 20–24 h and thus are normally not detected by traditional time-kill experiments. Another limitation of the use of bioluminescence is the needs of O_2 for the reaction that produce light. Studies have shown that O_2 diffusion can be limited in alginate gels and biofilms [30–32]. Its penetration is generally limited to 50–90 µm down from the surface of biofilms [30,33]. Thus oxygen diffusion can be a restriction for using bioluminescence with thick biofilms, as those formed on abiotic surfaces, or with large alginate beads [33], but for beads having diameters lower than 100 µm, oxygen diffusion limitation should not be responsible for a decrease in light production.

For adherent biofilms and planktonic cells, ATBs concentrations higher than the MIC induced a fast decrease of the luminescence. This decrease was faster and more intense for planktonic *PAO1* than for biofilms. Biofilm cells are less susceptible to antimicrobials than their planktonic counterparts [20,29,34]. Thus, the results obtained here are excepted if the bioluminescence correlates with the bacterial survival and metabolic state. The kinetics obtained with planktonic *PAO1*, adherent biofilms, and with *PAs* entrapped in both types of beads

displayed a concentration- and time-dependent change in luminescence with both ATBs. Time-kill curves with similar behaviors were established with planktonic *PAO1* treated with these two ATBs using the traditional bacterial counting method [35,36]. Except for TOB in calcium-alginate beads, ATBs concentrations around the MIC induced an initial decrease in luminescence that was followed by a rebound. In traditional time-kill experiments performed with these ATBs at these concentrations, a "regrowth" of the bacterial population is often observed [35,36]. This observation is generally attributed either to the adaptation of bacteria to the ATB (mutation) or to the selection of a subpopulation of bacteria that are already resistant but has a slower growth rate than the majority of the bacteria in normal condition. This luminescence rebound could be attributed to the growth of this kind of bacteria. For biofilms and for CIP concentrations between 0.25 and 0.5 times the MIC, a higher normalized luminescence value was observed at the plateau compared to the value obtained without ATB. This increase could be due to a stimulation of the bacterial metabolism by CIP, as observed by other studies that showed that sub-MIC CIP concentrations stimulate *PA* biofilm formation and virulence [37,38].

Agar and calcium-alginate beads are interchangeable for evaluating uncharged ATB such as the fluoroquinolone CIP, but not for cationic aminoglycosides such as TOB. Luminescence kinetics obtained in the presence of a large range of CIP concentrations (0–100 times the MIC) were virtually the same for *PAO1* trapped in calcium-alginate or agar beads. The size distributions of the two types of beads did not differ significantly, so their size should hardly influence the kinetic profiles. Therefore, both bead models seem interchangeable with CIP. For TOB however, a net difference was observed between kinetics obtained from *PAs* entrapped in agar and calcium-alginate beads. In alginate beads, *PAs* were up to 10 times less susceptible to TOB than in agar beads. In these experiments, beads were produced and immediately exposed to ATB. Initially, in these conditions, *PA*s entrapped are planktonic bacteria. Thus, at the beginning of the kinetics, the differences observed between the two types of beads cannot be attributed to phenomena such as the presence of low metabolically active bacteria found in biofilms. In addition, the effect of TOB on *PAs* entrapped freshly or for 2 days in agar beads prior to addition of TOB was almost similar for all tested TOB concentrations. This suggests that *PAO1* biofilm formed in agar beads had little effect on the TOB susceptibility compare to the effect of 2% m/v calcium-alginate. Thus, when using non-mucoid bacteria such as *PAO1* that do not produce alginate, the agar and calcium-alginate beads models are not interchangeable when testing cationic ATB such as TOB.

The calcium-alginate beads model was developed based on the finding that many *PA* found in CF patients are present as mucoid biofilms containing a large proportion of alginate in their EPS matrix. Numerous studies evaluating the effect of ATBs on these biofilms have shown that their efficacies are reduced compared to those obtained with free planktonic bacteria. Initially, it was thought that the ATBs tolerance of bacteria in these biofilms was due to the limitation of ATBs transport in biofilms due to the presence of the alginate-containing EPS matrix. [14,39,40]. So, the penetration of various ATBs within biofilms of different *PAs,* or within calcium-alginate gels made from commercial seaweed alginate or alginate from clinically relevant mucoid variants of *PA* was measured using various methods [14,39,41–43]. With the exception of some positively charged ATBs, such as aminoglycosides, which interact with negatively charged alginate [14,39,44–46] or calcium-alginate [39], most ATBs, including CIP, readily penetrated biofilms and alginate gels at sufficiently high velocities to exclude a limiting phenomenon that would contribute to antimicrobial tolerance [14,39,44]. Even though TOB penetration in alginate-based biofilms is delayed [42], some studies considered to have a minor effect on the ATB tolerance [47]. In our study, the effective diffusivity of CIP at 37 °C calculated from transport experiments through both gels was around 1.5×10^{-6} cm^2/s, which is 5 times lower than its value in water [16]. Even with this reduction, luminescence kinetics obtained in the presence of CIP with both types of beads were highly similar to those obtained with planktonic bacteria. TOB effective diffusivity in agar ($1.6 \pm 0.7 \times 10^{-6}$ cm^2/s) was close to that of the CIP in this gel and was reduced by 3.5 fold in relation to its diffusivity in water. This effective diffusivity was 2 times lower than the value found by Gordon et al. [39] in a similar 2% m/v agar gels (3.0×10^{-6} cm^2/s). TOB effective diffusivity in 2% (m/v) calcium-alginate gel ($0.8 \pm 0.5 \times 10^{-6}$ cm^2/s) was 2 times lower than in 2% (m/v) agar gel and 7 times lower than in water [16]. This value was in the same range than the value found by Gordon et al. [39] in 2% (m/v) alginate containing calcium lactate as a gelling agent ($0.65 \pm \times 10^{-6}$ cm^2/s). TOB diffusivity in the calcium-alginate gel was also assessed from its binding at equilibrium to this gel as described by Nichols *et al.* [14]. It was evaluated at 1.2×10^{-6} cm^2/s, which is in the same range of values as calculated from the transport experiment across a calcium-alginate gel layer. According to Stewart [47] and Nichols et al. [14], the time required for a molecule to achieve 90% of the dispersing medium concentration at the center of a spherical polymer bead is estimated by $t_{90} = 0.37 \times R^2/De$, where R is the radius of the bead and *De* is the effective diffusivity of the molecule in the polymer. Therefore, with a diffusivity of $0.8 \pm 0.5 \times 10^{-6}$ cm^2/s and beads having a maximal diameter of 100 μm, 12 s should be needed for TOB to obtain 90% of the dispersing medium concentration at the center of beads. Thus, only a decrease in the diffusivity of TOB in alginate by a factor of 1000–10,000 could explain by itself the difference in efficacy against *PAO1* entrapped in calcium-alginate compared with those trapped in agar.

The reduction of TOB diffusivity seems not a major mechanism of TOB resistance of *PA* in calcium-alginate beads. However, several studies proposed that the delay in TOB penetration give to the bacteria the time to adapt to the ATB and adopt a more antimicrobial-tolerant state before killing concentrations of the ATB can be achieved [48]. In agreement with this suggestion, hydrolysis of alginate by alginate lyase enhanced the activity of TOB in biofilms by dissolving the biofilm matrix [49]. Also, PA exposures to sub-lethal concentrations of TOB results in phenotypic alterations such as increased EPS productions or activation of ATB efflux pump [50].

Alginate beads dispersed in artificial sputum media could be a good model to simulate pulmonary biofilms. In cystic fibrosis (CF) patients, the conductive zone serves as a bacterial reservoir where the bacteria are organized in mucoid biofilms within the mucus, protected against ATBs and host defenses [5]. These two gels that are biofilm and mucus are formed of negatively charged polymers that could behave as barrier able to reversibly bind cationic ATBs and slow down their penetration [12,51]. This reduction in ATBs penetration rate could give the bacteria enough time to adapt to the ATBs [40,48]. *In vivo PA* biofilm patches found in the pulmonary mucus of chronically infected CF patients have sizes ranged from 5 to 200 μm in diameter [5,18,52]. With a high frequency, *PAs* found in these infections are able to create mucoid biofilms having a high concentration in alginate [34]. Thus, alginate beads having the size of the biofilm clusters found in the CF patients lungs dispersed in mucus or mucus-simulating medium could be a good model for evaluating anti-biofilm strategies. In the present study, we have shown that the dispersion of the alginate beads in ASM further reduced the efficacy of TOB compared to the same beads dispersed in MHB. This result is in agreement with Müller et al. [45] study showing a significant reduction of TOB efficacy against *PA* biofilms grown on 96-well plates in the presence of mucus compared with those grown in the absence of mucus. Also, several studies have shown that the presence of mucus altered the *PA* biofilms behaviors [53] and promote the expression of several genes responsible for ATB resistance [54,55].

In human, most planktonic bacteria are killed by the ATB and the residual bacteria are eradicated by the immune system. For biofilms, however, due to the presence of the EPS matrix, immune cells cannot reach the bacteria and the residual cells that are not killed by the ATB might be able to restore the biofilm. Also, bacteria in biofilms are less susceptible to ATBs than their planktonic counterparts. Therefore, ATB

concentrations required to eradicate bacterial infections with biofilms are higher than the clinical targets usually used to treat infections caused by planktonic cells. These concentrations are difficultly achievable via systemic administration and pulmonary biofilms eradication seems only possible by ATB inhalation due to the possibility to achieve high ATB concentrations in biofilms while avoiding side effects and toxicity. The mucus barrier is often neglected in *in vitro* tests employed to evaluate the efficacy of inhaled ATBs. This model could be highly relevant in testing the efficacy of inhaled ATB, whose development to treat pulmonary lung infections is increasing [21,56].

In CF patients, activated polymorphonuclear leukocytes (PMNs) are accumulating around the bacterial aggregates [5]. PMNs impact on *PAs* behavior and release a large amount of extracellular DNA that could affect cationic ATB efficacy [57,58]. Thus, a model using small beads of calcium-alginate dispersed in medium simulating mucus could be supplemented with immune cell lines that could aggregate around the beads, which would make it possible to study the effect of the three barriers (biofilm, mucus, and agglomerated immune cells) that an ATB must pass to reach the bacteria.

5. Conclusion

These results show that the agar and alginate beads models can be interchangeable only for uncharged ATB, such as CIP, but not for all ATB. In vitro experiments performed in this study could be a quick way to evaluate the influence of each model on a given ATB before performing animal experiments.

Acknowledgements

This work was supported by internal research funds of the University of Poitiers and INSERM.

Appendix A. Supplementary material

Supplementary data to this article can be found online at https://doi.org/10.1016/j.ejpb.2019.08.006.

References

[1] H. Cash, D. Woods, B. McCullough, W. Johanson Jr., J. Bass, A rat model of chronic respiratory infection with Pseudomonas aeruginosa, Am. Rev. Respirat. Disease 119 (1979) 453–459.
[2] E. Growcott, A. Coulthard, R. Amison, E. Hardaker, V. Saxena, L. Malt, P. Jones, A. Grevot, C. Poll, C. Osborne, Characterisation of a refined rat model of respiratory infection with Pseudomonas aeruginosa and the effect of ciprofloxacin, J. Cyst. Fibros. 10 (2011) 166–174.
[3] J. Lam, R. Chan, K. Lam, J. Costerton, Production of mucoid microcolonies by Pseudomonas aeruginosa within infected lungs in cystic fibrosis, Infect. Immun. 28 (1980) 546–556.
[4] B.G.S. Torres, V.E. Helfer, P.M. Bernardes, A.J. Macedo, E.I. Nielsen, L.E. Friberg, T. Dalla Costa, Population pharmacokinetic modeling as a tool to characterize the decrease in ciprofloxacin free interstitial levels caused by pseudomonas aeruginosa biofilm lung infection in wistar rats, Antimicrob. Agents Chemother. 61 (2017) e02553–02516.
[5] T. Bjarnsholt, P.Ø. Jensen, M.J. Fiandaca, J. Pedersen, C.R. Hansen, C.B. Andersen, T. Pressler, M. Givskov, N. Høiby, Pseudomonas aeruginosa biofilms in the respiratory tract of cystic fibrosis patients, Pediatr. Pulmonol. 44 (2009) 547–558.
[6] H. Bayes, N. Ritchie, S. Irvine, T. Evans, A murine model of early Pseudomonas aeruginosa lung disease with transition to chronic infection, Sci. Rep. 6 (2016) 1–10.
[7] S. Gandi, I. Cranston, G. Mclachlan, S. Wright, J. Baily, S. Stimpson, S. Madden, M. Whitmarsh, A. Young, M. Mcelroy, Effects of direct lung dosing of Tobramycin in a rat chronic infection model using Pseudomonas aeruginosa RP73, Eur. Respir. J. 52 (2018) 2656.
[8] W. Hengzhuang, K. Green, T. Pressler, M. Skov, T.L. Katzenstein, X. Wu, N. Høiby, Optimization of colistin dosing regimen for cystic fibrosis patients with chronic Pseudomonas aeruginosa biofilm lung infections, Pediatr. Pulmonol. 54 (2019) 575–580.
[9] D.-J. Kim, S.-G. Chung, S.-H. Lee, J.-W. Choi, Relation of microbial biomass to counting units for Pseudomonas aeruginosa, Afric. J. Microbiol. Res. 6 (2012) 4620–4622.
[10] T. Jouenne, O. Tresse, G.-A. Junter, Agar-entrapped bacteria as an in vitro model of biofilms and their susceptibility to antibiotics, FEMS Microbiol. Lett. 119 (1994) 237–242.
[11] A. Braun, K. Sewald, L. Müller, S. Wronski, X. Murgia, C.-M. Lehr, C. Börger, L. Siebenbürger, M. Hittinger, K. Schwarzkopf, S. Häussler, Human airway mucus alters susceptibility of Pseudomonas aeruginosa biofilms to tobramycin, but not colistin, J. Antimicrob. Chemother. 73 (2018) 2762–2769.
[12] T.F. Bahamondez-Canas, H. Zhang, F. Tewes, J. Leal, H.D. Smyth, PEGylation of tobramycin improves mucus penetration and antimicrobial activity against Pseudomonas aeruginosa biofilms in vitro, Mol. Pharm. 15 (2018) 1643–1652.
[13] S.D. Dinesh, Artificial sputum medium, Protoc. exch, 2010.
[14] W. Nichols, S. Dorrington, M. Slack, H. Walmsley, Inhibition of tobramycin diffusion by binding to alginate, Antimicrob. Agents Chemother. 32 (1988) 518–523.
[15] S. Marchand, N. Grégoire, J. Brillault, I. Lamarche, P. Gobin, W. Couet, Biopharmaceutical characterization of nebulized antimicrobial agents in rats: 3. Tobramycin, Antimicrob. Agents Chemother. 59 (2015) 6646–6647.
[16] P.S. Stewart, Theoretical aspects of antibiotic diffusion into microbial biofilms, Antimicrob. Agents Chemother. 40 (1996) 2517–2522.
[17] N. Høiby, O. Ciofu, T. Bjarnsholt, Pseudomonas aeruginosa biofilms in cystic fibrosis, Future Microbiol. 5 (2010) 1663–1674.
[18] T. Bjarnsholt, The role of bacterial biofilms in chronic infections, Apmis 121 (2013) 1–58.
[19] K.M. Langan, T. Kotsimbos, A.Y. Peleg, Managing Pseudomonas aeruginosa respiratory infections in cystic fibrosis, Curr. Opin. Infect. Diseases 28 (2015) 547–556.
[20] H. Wu, C. Moser, H.-Z. Wang, N. Høiby, Z.-J. Song, Strategies for combating bacterial biofilm infections, Int. J. Oral Sci. 7 (2014) 1.
[21] N. Günday Türeli, A. Torge, J. Juntke, B.C. Schwarz, N. Schneider-Daum, A.E. Türeli, C.-M. Lehr, M. Schneider, Ciprofloxacin-loaded PLGA nanoparticles against cystic fibrosis P. aeruginosa lung infections, Eur. J. Pharm. Biopharm. 117 (2017) 363–371.
[22] J. Ernst, M. Klinger-Strobel, K. Arnold, J. Thamm, A. Hartung, M.W. Pletz, O. Makarewicz, D. Fischer, Polyester-based particles to overcome the obstacles of mucus and biofilms in the lung for tobramycin application under static and dynamic fluidic conditions, Eur. J. Pharm. Biopharm. 131 (2018) 120–129.
[23] B. Lamy, F. Tewes, D.R. Serrano, I. Lamarche, P. Gobin, W. Couet, A.M. Healy, S. Marchand, New aerosol formulation to control ciprofloxacin pulmonary concentration, J. Control. Release 271 (2018) 118–126.
[24] H. Bandara, M. Herpin, D. Kolacny Jr., A. Harb, D. Romanovicz, H. Smyth, Incorporation of farnesol significantly increases the efficacy of liposomal ciprofloxacin against Pseudomonas aeruginosa biofilms in vitro, Mol. Pharm. 13 (2016) 2760–2770.
[25] R. Thorn, S. Nelson, J. Greenman, Use of a bioluminescent Pseudomonas aeruginosa strain within an in vitro microbiological system, as a model of wound infection, to assess the antimicrobial efficacy of wound dressings by monitoring light production, Antimicrob. Agents Chemother. 51 (2007) 3217–3224.
[26] C.N.H. Marques, S.M. Nelson, Pharmacodynamics of ciprofloxacin against Pseudomonas aeruginosa planktonic and biofilm-derived cells, Lett. Appl. Microbiol. 68 (2019) 350–359.
[27] C.N. Marques, V.C. Salisbury, J. Greenman, K.E. Bowker, S.M. Nelson, Discrepancy between viable counts and light output as viability measurements, following ciprofloxacin challenge of self-bioluminescent Pseudomonas aeruginosa biofilms, J. Antimicrob. Chemother. 56 (2005) 665–671.
[28] C. Fux, J.W. Costerton, P.S. Stewart, P. Stoodley, Survival strategies of infectious biofilms, Trends Microbiol. 13 (2005) 34–40.
[29] P.S. Stewart, Mechanisms of antibiotic resistance in bacterial biofilms, Int. J. Med. Microbiol. 292 (2002) 107–113.
[30] M. Sønderholm, K.N. Kragh, K. Koren, T.H. Jakobsen, S.E. Darch, M. Alhede, P.Ø. Jensen, M. Whiteley, M. Kühl, T. Bjarnsholt, Pseudomonas aeruginosa aggregate formation in an alginate bead model system exhibits in vivo-like characteristics, Appl. Environ. Microbiol. 83 (2017) e00113–00117.
[31] D.J. Hassett, Anaerobic production of alginate by Pseudomonas aeruginosa: alginate restricts diffusion of oxygen, J. Bacteriol. 178 (1996) 7322–7325.
[32] B. Pabst, B. Pitts, E. Lauchnor, P.S. Stewart, Gel-entrapped Staphylococcus aureus bacteria as models of biofilm infection exhibit growth in dense aggregates, oxygen limitation, antibiotic tolerance, and heterogeneous gene expression, Antimicrob. Agents Chemother. 60 (2016) 6294–6301.
[33] M. Sønderholm, K. Koren, D. Wangpraseurt, P.Ø. Jensen, M. Kolpen, K.N. Kragh, T. Bjarnsholt, M. Kühl, Tools for studying growth patterns and chemical dynamics of aggregated Pseudomonas aeruginosa exposed to different electron acceptors in an alginate bead model, npj Biofilms Microbiomes 4 (2018) 3.
[34] N. Høiby, T. Bjarnsholt, M. Givskov, S. Molin, O. Ciofu, Antibiotic resistance of bacterial biofilms, Int. J. Antimicrob. Agents 35 (2010) 322–332.
[35] J.B. Bulitta, N.S. Ly, C.B. Landersdorfer, N.A. Wanigaratne, T. Velkov, R. Yadav, A. Oliver, L. Martin, B.S. Shin, A. Forrest, B.T. Tsuji, Two mechanisms of killing of *Pseudomonas aeruginosa* by Tobramycin assessed at multiple inocula via mechanism-based modeling, Antimicrob. Agents Chemother. 59 (2015) 2315–2327.
[36] N. Grégoire, S. Raherison, C. Grignon, E. Comets, M. Marliat, M.-C. Ploy, W. Couet, Semimechanistic pharmacokinetic-pharmacodynamic model with adaptation development for time-kill experiments of ciprofloxacin against Pseudomonas aeruginosa, Antimicrob. Agents Chemother. 54 (2010) 2379–2384.
[37] J.F. Linares, I. Gustafsson, F. Baquero, J. Martinez, Antibiotics as intermicrobial signaling agents instead of weapons, Proc. Natl. Acad. Sci. 103 (2006) 19484–19489.
[38] F. Tewes, T.F. Bahamondez-Canas, H.D.C. Smyth, Efficacy of ciprofloxacin and its copper complex against Pseudomonas aeruginosa biofilms, AAPS PharmSciTech 20 (2019) 205–214.

[39] C.A. Gordon, N.A. Hodges, C. Marriott, Antibiotic interaction and diffusion through alginate and exopolysaccharide of cystic fibrosis-derived Pseudomonas aeruginosa, J. Antimicrob. Chemother. 22 (1988) 667–674.
[40] B.S. Tseng, W. Zhang, J.J. Harrison, T.P. Quach, J.L. Song, J. Penterman, P.K. Singh, D.L. Chopp, A.I. Packman, M.R. Parsek, The extracellular matrix protects Pseudomonas aeruginosa biofilms by limiting the penetration of tobramycin, Environ. Microbiol. 15 (2013) 2865–2878.
[41] M. Shigeta, G. Tanaka, H. Komatsuzawa, M. Sugai, H. Suginaka, T. Usui, Permeation of antimicrobial agents through Pseudomonas aeruginosa biofilms: a simple method, Chemotherapy 43 (1997) 340–345.
[42] M.C. Walters, F. Roe, A. Bugnicourt, M.J. Franklin, P.S. Stewart, Contributions of antibiotic penetration, oxygen limitation, and low metabolic activity to tolerance of Pseudomonas aeruginosa biofilms to ciprofloxacin and tobramycin, Antimicrob. Agents Chemother. 47 (2003) 317–323.
[43] L. Coquet, G. Junter, T. Jouenne, Resistance of artificial biofilms of Pseudomonas aeruginosa to imipenem and tobramycin, J. Antimicrob. Chemother. 42 (1998) 755–760.
[44] R.A. Hatch, N.L. Schiller, Alginate lyase promotes diffusion of aminoglycosides through the extracellular polysaccharide of MucoidPseudomonas aeruginosa, Antimicrob. Agents Chemother. 42 (1998) 974–977.
[45] L. Müller, X. Murgia, L. Siebenbürger, C. Börger, K. Schwarzkopf, K. Sewald, S. Häussler, A. Braun, C.-M. Lehr, M. Hittinger, Human airway mucus alters susceptibility of Pseudomonas aeruginosa biofilms to tobramycin, but not colistin, J. Antimicrob. Chemother. 73 (2018) 2762–2769.
[46] M. Heriot, B. Nottelet, X. Garric, M. D'Este, G.R. Richards, F.T. Moriarty, D. Eglin, O. Guillaume, Interaction of gentamicin sulfate with alginate and consequences on the physico-chemical properties of alginate-containing biofilms, Int. J. Biol. Macromol. 121 (2019) 390–397.
[47] P.S. Stewart, Diffusion in biofilms, J. Bacteriol. 185 (2003) 1485–1491.
[48] B. Cao, L. Christophersen, M. Kolpen, P.Ø. Jensen, K. Sneppen, N. Høiby, C. Moser, T. Sams, Diffusion retardation by binding of tobramycin in an alginate biofilm model, PLoS ONE 11 (2016) e0153616.
[49] M. Alipour, Z.E. Suntres, A. Omri, Importance of DNase and alginate lyase for enhancing free and liposome encapsulated aminoglycoside activity against Pseudomonas aeruginosa, J. Antimicrob. Chemother. 64 (2009) 317–325.
[50] L.R. Hoffman, D.A. D'Argenio, M.J. MacCoss, Z. Zhang, R.A. Jones, S.I. Miller, Aminoglycoside antibiotics induce bacterial biofilm formation, Nature 436 (2005) 1171–1175.
[51] J. Witten, T. Samad, K. Ribbeck, Molecular characterization of mucus binding, Biomacromolecules 20 (2019) 1505–1513.
[52] T. Bjarnsholt, M. Alhede, M. Alhede, S.R. Eickhardt-Sørensen, C. Moser, M. Kühl, P.Ø. Jensen, N. Høiby, The in vivo biofilm, Trends Microbiol. 21 (2013) 466–474.
[53] C.L. Haley, J.A. Colmer-Hamood, A.N. Hamood, Characterization of biofilm-like structures formed by Pseudomonas aeruginosa in a synthetic mucus medium, BMC Microbiol. 12 (2012) 181.
[54] R.M. Landry, D. An, J.T. Hupp, P.K. Singh, M.R. Parsek, Mucin-Pseudomonas aeruginosa interactions promote biofilm formation and antibiotic resistance, Mol. Microbiol. 59 (2006) 142–151.
[55] S. Lory, S. Jin, J.M. Boyd, J.L. Rakeman, P. Bergman, Differential gene expression by Pseudomonas aeruginosa during interaction with respiratory mucus, Am. J. Respir. Crit. Care Med. 154 (1996) S183.
[56] P.P.H. Le Brun, A.H. de Boer, G.P.M. Mannes, D.M.I. de Fraîture, R.W. Brimicombe, D.J. Touw, A.A. Vinks, H.W. Frijlink, H.G.M. Heijerman, Dry powder inhalation of antibiotics in cystic fibrosis therapy: part 2: Inhalation of a novel colistin dry powder formulation: a feasibility study in healthy volunteers and patients, Eur. J. Pharm. Biopharm. 54 (2002) 25–32.
[57] W.-C. Chiang, M. Nilsson, P.Ø. Jensen, N. Høiby, T.E. Nielsen, M. Givskov, T. Tolker-Nielsen, Extracellular DNA shields against aminoglycosides in Pseudomonas aeruginosa biofilms, Antimicrob. Agents Chemother. 57 (2013) 2352–2361.
[58] H. Mulcahy, L. Charron-Mazenod, S. Lewenza, Extracellular DNA chelates cations and induces antibiotic resistance in Pseudomonas aeruginosa biofilms, PLoS Pathog. 4 (2008) e1000213.